Corresponding author mail id : a.altmann@ucl.ac.uk

# Event-based modelling in temporal lobe epilepsy demonstrates progressive atrophy from cross-sectional data

Seymour M. Lopez[1], Leon M. Aksman[1,2], Neil P. Oxtoby[3], Sjoerd B. Vos[1,4], Jun Rao[5], Erik Kaestner[5], Saud Alhusaini[6,7], Marina Alvim[8], Benjamin Bender[9], Andrea Bernasconi[10], Neda Bernasconi[10], Boris Bernhardt[11], Lorenzo Caciagli[11,12], Benoit Caldairou[10], Maria Eugenia Caligiuri[13], Angels Calvet[14], Fernando Cendes[8], Luis Concha[15], Estefania Conde-Blanco[16,17], Esmaeil Davoodi-Bojd[18], Christophe de Bézenac[19], Norman Delanty[7,20], Patricia M. Desmond[21], Orrin Devinsky[22], Martin Domin[23], John S. Duncan[12,24], Niels K. Focke[25], Sonya Foley[26], Francesco Fortunato[27], Marian Galovic[12,28], Antonio Gambardella[13,27], Ezequiel Gleichgerrcht[29], Renzo Guerrini[30], Khalid Hamandi[26,31], Victoria Ives-Deliperi[32], Graeme D. Jackson[33–35], Neda Jahanshad[36], Simon S. Keller[37], Peter Kochunov[38], Raviteja Kotikalapudi[9,39,40], Barbara A.K. Kreilkamp[37,41], Angelo Labate[13,27], Sara Larivière[11], Matteo Lenge[42,43], Elaine Lui[21], Charles Malpas[44,45], Pascal Martin[40], Mario Mascalchi[46], Sarah E. Medland[47], Stefano Meletti[48,49], Marcia E. Morita-Sherman[50,51], Thomas W. Owen[52], Mark Richardson[53], Antonella Riva[54,55], Theodor Rüber[56], Ben Sinclair[57,58], Hamid Soltanian-Zadeh[18,59], Dan J. Stein[60], Pasquale Striano[54,55], Peter N. Taylor[12,52], Sophia I. Thomopoulos[36], Paul M. Thompson[36], Manuela Tondelli[48,61], Anna Elisabetta Vaudano[48,49], Lucy Vivash[57,58], Yujiang Wang[12,52], Bernd Weber[62], Christopher D. Whelan[7], Roland Wiest[63], Gavin P. Winston[12,24,64], Clarissa Lin Yasuda[8], Carrie R. McDonald[5], Daniel C. Alexander[3], Sanjay M. Sisodiya[12,24], Andre Altmann[1] for the ENIGMA-Epilepsy Working Group*

Consortium banner:

*Núria Bargalló[14,65,66], Emanuele Bartolini[30], Terence J. O'Brien[45,57], Rhys H. Thomas[67]

Affiliations

1. Centre for Medical Image Computing, Department of Medical Physics and Biomedical Engineering, University College London, London, UK.
2. Stevens Neuroimaging and Informatics Institute, Keck School of Medicine, University of Southern California, Los Angeles, CA, USA.

This article has been accepted for publication and undergone full peer review but has not been through the copyediting, typesetting, pagination and proofreading process, which may lead to differences between this version and the Version of Record. Please cite this article as doi: 10.1111/epi.17316

3. Centre for Medical Image Computing, Department of Computer Science, University College London, London, UK.
4. Neuroradiological Academic Unit, UCL Queen Square Institute of Neurology, University College London, London, UK.
5. Department of Psychiatry, University of California San Diego, La Jolla, CA, USA.
6. Department of Neurology, Alpert Medical School of Brown University, Providence, RI, USA.
7. Department of Molecular and Cellular Therapeutics, The Royal College of Surgeons in Ireland, Dublin, Ireland.
8. Department of Neurology and Neuroimaging Laboratory, University of Campinas - UNICAMP, Campinas, SP, Brazil.
9. Department of Radiology, Diagnostic and Interventional Neuroradiology, University Hospital Tübingen, Tübingen, Germany.
10. Neuroimaging of Epilepsy Laboratory, Montreal Neurological Institute, McGill University, Montreal, QC, Canada.
11. Multimodal Imaging and Connectome Analysis Laboratory, McConnell Brain Imaging Centre, Montreal Neurological Institute and Hospital, McGill University, Montreal, QC, Canada.
12. Department of Clinical and Experimental Epilepsy, UCL Queen Square Institute of Neurology, London, WC1N 3BG, UK.
13. Neuroscience Research Center, Department of Medical and Surgical Sciences, University "Magna Græcia" of Catanzaro, Catanzaro, Italy.
14. Magnetic Resonance Image Core Facility, Institut d'Investigacions Biomèdiques August Pi i Sunyer (IDIBAPS), Universitat de Barcelona, Barcelona, Spain.
15. Instituto de Neurobiología, Universidad Nacional Autónoma de México, Querétaro, Mexico.
16. Epilepsy Program, Neurology Department, Hospital Clínic de Barcelona, Barcelona, Spain.
17. Institut D'Investigacions Biomèdiques August Pi i Sunyer (IDIBAPS), Barcelona, Spain.
18. Radiology and Research Administration, Henry Ford Health System, Detroit, MI, USA.
19. Department of Pharmacology and Therapeutics, Institute of Systems, Molecular and Integrative Biology, University of Liverpool, Liverpool, UK.
20. FutureNeuro SFI Research Centre for Rare and Chronic Neurological Diseases, Dublin,

Ireland.
21. Department of Radiology, The Royal Melbourne Hospital, University of Melbourne, Melbourne, VIC, Australia.
22. New York University Grossman School of Medicine, New York City, NY, USA.
23. Functional Imaging Unit, Department of Diagnostic Radiology and Neuroradiology, University Medicine Greifswald, Greifswald, Germany.
24. Chalfont Centre for Epilepsy, Chalfont St Peter, Bucks, UK.
25. Department of Neurology, University Medical Center, Göttingen, Germany.
26. Cardiff University Brain Research Imaging Centre, School of Psychology, Cardiff University, Cardiff, UK.
27. Institute of Neurology, Department of Medical and Surgical Sciences, University "Magna Græcia" of Catanzaro, Catanzaro, Italy.
28. Department of Neurology, University Hospital Zurich, Zurich, Switzerland.
29. Department of Neurology, Medical University of South Carolina, Charleston, SC, USA.
30. Neuroscience Department, University of Florence, Florence, Italy.
31. The Wales Epilepsy Unit, Department of Neurology, University Hospital of Wales, Cardiff, UK.
32. Neuroscience Institute, University of Cape Town, Cape Town, South Africa.
33. Florey Institute of Neuroscience and Mental Health, Austin Campus, Heidelberg, VIC, Australia.
34. University of Melbourne, Parkville, VIC, Australia.
35. Department of Neurology, Austin Health, Heidelberg, VIC, Australia.
36. Imaging Genetics Center, Mark and Mary Stevens Neuroimaging and Informatics Institute, Keck School of Medicine, University of Southern California, Marina del Rey, CA, USA.
37. Institute of Systems, Molecular and Integrative Biology, University of Liverpool, Liverpool, UK.
38. Department of Psychiatry University of Maryland School of Medicine, Baltimore, MD, USA.
39. Department of Clinical Neurophysiology, University Hospital Göttingen, Goettingen, Germany.
40. Department of Neurology and Epileptology, Hertie Institute for Clinical Brain Research, University of Tübingen, Tübingen, Germany.

41. University Medicine Göttingen, Clinical Neurophysiology, Göttingen, Germany.
42. Pediatric Neurology, Neurogenetics and Neurobiology Unit and Laboratories, Children's Hospital A. Meyer-University of Florence, Florence, Italy.
43. Functional and Epilepsy Neurosurgery Unit, Neurosurgery Department, Children's Hospital A. Meyer-University of Florence, Florence, Italy.
44. Department of Neurology, The Royal Melbourne Hospital, Melbourne, VIC, Australia.
45. The Department of Medicine, The Royal Melbourne Hospital, The University of Melbourne, Parkville, VIC, Australia.
46. 'Mario Serio' Department of Clinical and Experimental Medica Sciences, University of Florence, Florence, Italy.
47. Psychiatric Genetics, QIMR Berghofer Medical Research Institute, Brisbane, QLD, Australia.
48. Department of Biomedical, Metabolic, and Neural Sciences, University of Modena and Reggio Emilia, Modena, Italy.
49. Neurology Unit, OCB Hospital, Azienda Ospedaliera-Universitaria Modena, Modena, Italy.
50. Department of Neurology, University of Campinas - UNICAMP, Campinas, SP, Brazil.
51. Cleveland Clinic Neurological Institute, Cleveland, USA.
52. School of Computing, Newcastle University, Newcastle upon Tyne, UK.
53. Division of Neuroscience, King's College London, London, UK.
54. IRCCS Istituto 'Giannina Gaslini', Genova, Italy.
55. Department of Neurosciences, Rehabilitation, Ophthalmology, Genetics, Maternal and Child Health, University of Genova, Genova, Italy.
56. Department of Epileptology, University Hospital Bonn, Bonn, Germany.
57. Department of Neuroscience, Central Clinical School, Alfred Hospital, Monash University, Melbourne, VIC, Australia.
58. Departments of Medicine and Radiology, The Royal Melbourne Hospital, The University of Melbourne, Parkville, VIC, Australia.
59. School of Electrical and Computer Engineering, College of Engineering, University of Tehran, Tehran, Iran.
60. SA MRC Unit on Risk & Resilience in Mental Disorders, Dept of Psychiatry & Neuroscience Institute, University of Cape Town, Cape Town, South Africa.
61. Primary Care Department, Azienda Sanitaria Locale di Modena, Modena, Italy.

62. Institute of Experimental Epileptology and Cognition Research, University of Bonn, Bonn, Germany.
63. Support Center for Advanced Neuroimaging, University Institute of Diagnostic and Interventional Neuroradiology, Inselspital, Bern University Hospital, University of Bern, Bern, Switzerland.
64. Department of Medicine, Division of Neurology, Queen's University, Kingston, ON, Canada
65. Department of Radiology of Center of Image Diagnosis (CDIC), Hospital Clinic de Barcelona, Barcelona, Spain.
66. Centro Investigación Biomédica en Red de Salud Mental (CIBERSAM), Madrid, Spain.
67. Institute of Translational and Clinical Research, Newcastle University, Newcastle upon Tyne, UK.

*Abstract*

**Objective:** Recent work has shown that people with common epilepsies have characteristic patterns of cortical thinning, and that these changes may be progressive over time. Leveraging a large multi-centre cross-sectional cohort, we investigated whether regional morphometric changes occur in a sequential manner, and whether these changes in people with mesial temporal lobe epilepsy and hippocampal sclerosis (MTLE-HS) correlate with clinical features.

**Methods:** We extracted regional measures of cortical thickness, surface area and subcortical brain volumes from T1-weighted (T1W) MRI scans collected by the ENIGMA-Epilepsy consortium, comprising 804 people with MTLE-HS and 1,625 healthy controls from 25 centres. Features with a moderate case-control effect size (Cohen's d≥0.5) were used to train an Event-Based Model (EBM), which estimates a sequence of disease-specific biomarker changes from cross-sectional data and assigns a biomarker-based fine-grained disease stage to individual patients. We tested for associations between EBM disease stage and duration of epilepsy, age of onset and anti-seizure medicine (ASM) resistance.

**Results:** In MTLE-HS, decrease in ipsilateral hippocampal volume along with increased asymmetry in hippocampal volume was followed by reduced thickness in neocortical regions, reduction in ipsilateral thalamus volume and, finally, increase in ipsilateral lateral ventricle volume. EBM stage was correlated to duration of illness (Spearman's $\rho$=0.293, $p$=7.03x10$^{-16}$), age of onset ($\rho$=-0.18, $p$=9.82x10$^{-7}$) and ASM resistance (AUC=0.59, $p$=0.043, Mann-Whitney U test). However, associations were driven by cases assigned to EBM stage zero, which represents MTLE-HS with mild or non-detectable abnormality on T1W MRI.

**Significance:** From cross-sectional MRI, we reconstructed a disease progression model that highlights a sequence of MRI changes that aligns with previous longitudinal studies.
This model could be used to stage MTLE-HS subjects in other cohorts and help establish connections between imaging-based progression staging and clinical features.

*Keywords*

*MTLE, event-based model, disease progression, patient staging, duration of illness*

*Key Points*

- We estimated the sequence of progression of subcortical and neocortical atrophy in medial temporal lobe epilepsy (MTLE) with hippocampal sclerosis (HS).
- Abnormality started in the hippocampus, followed by decreased cortical thickness in the parietal and frontal lobes, thalamic volume and ventricular expansion.
- Image-based disease stages were correlated with duration of illness, age of onset and drug resistance.
- Associations were driven by MTLE-HS cases showing mild volume loss in the ipsilateral hippocampus that was indistinguishable from variation in the control group.

Word Count: 3,979

## *1. Introduction*

Epilepsy is characterized by recurrent seizures caused by excessive and abnormal neuronal activity in the cortex. Moreover, there is consistent evidence indicating decreased grey matter volume in people with epilepsy (PWE) compared to healthy controls. Quantitative analysis of MRI data from PWE in a large multicentre cohort showed reduced cortical thickness and subcortical volume in specific brain regions according to epilepsy type (Whelan et al., 2018). In people with focal epilepsy, differences tend to be more pronounced ipsilateral to the seizure focus (Park et al., 2021; Whelan et al., 2018). Beyond cortical thickness and subcortical volume differences, surface area reduction in the mesial and anterior temporal cortex has been previously reported (Alhusaini et al., 2012).

Whether seizures, anti-seizure medication (ASM), head injuries, the epileptogenic process, the maintenance of seizure occurrence, or other comorbidities cause the observed loss of brain tissue is a much-discussed question. Many studies have found that grey matter thickness is correlated with the duration of illness in the common epilepsies, indicating that these cross-sectional differences may be progressive (Bernasconi et al., 2005; Bernhardt et al., 2009; Bonilha et al., 2006; Coan et al., 2009; Whelan et al., 2018). Deciphering how grey matter reductions unfold over time in epilepsy is of great importance, but progress has been limited by the scarcity of longitudinal imaging cohorts. Recent work in this field has leveraged advanced mathematical models to infer longitudinal atrophy patterns from cross-sectional data. For instance, in a dataset of people with mesial temporal lobe epilepsy (MTLE), Zhang et al. used Granger causality analysis to determine whether a previously affected region, or a group of regions, helped to predict the next brain region to exhibit atrophy; they found that subcortical regions such as the hippocampus and thalamus causally affected other regions, most prominently the prefrontal cortex and cerebellum (Zhang et al., 2017). This approach, however, does not allow direct inference of a temporal sequence. A major step towards addressing the question of progression was provided by previous longitudinal studies that assessed progressive atrophy in patients with TLE (Bernhardt et al., 2009; Bernhardt et al., 2013; Coan et al., 2009), and prior meta-analytical studies on the topic (Caciagli et al., 2017). One recent study investigated people with focal epilepsy and longitudinal MRI scans at least six months apart, showing that the annualized rate of atrophy within brain regions structurally connected to the ipsilateral hippocampus exceeded the rate associated with healthy aging (Galovic et al., 2019); whilst they demonstrated the progressive nature of atrophy,

their approach did not address whether there is an explicit sequence in which these structural changes occur or whether this sequence can be used to stage epilepsy. Moreover, lower hippocampal volume has been reported in non-affected siblings and thus may reflect a genetic origin (Kobayashi et al., 2002; Long et al., 2020; Tsai et al., 2013; Vaughan et al., 2017) predating any further changes such as cortical thinning, which was not observed in siblings (Alhusaini et al., 2019). We surmise that staging epilepsy in patients using a single MRI scan will help future research to assess the effectiveness of anti-seizure medications (ASMs) and disease-modifying agents, e.g., by directly establishing a link between disease stage and drug response or by improving efficacy of inclusion criteria for clinical trials of ASM candidates. Furthermore, understanding the spatial progression of atrophy in MTLE could help answer questions such as whether unilateral MTLE with hippocampal sclerosis (HS) can lead to bilateral HS in an individual patient.

In this work, we investigated disease progression in patients with radiographically identified sclerosis of the hippocampus or the mesial temporal lobe (MTLE-HS) using the event-based model (EBM). In brief, the EBM is a machine learning approach that learns the most likely ordering of biomarker changes from cross-sectional data. The EBM was originally developed to study progressive loss of brain tissue in Alzheimer's and Huntington's diseases (Fonteijn et al., 2012). A trained EBM can be used to assign a disease stage to each patient based on their atrophy pattern (Young et al., 2014). Since it was introduced, the EBM has been used across a wide range of neurological diseases, including multiple sclerosis (Dekker et al., 2021; Eshaghi et al., 2018), amyotrophic lateral sclerosis (Gabel et al., 2020) and Parkinson's disease (Oxtoby et al., 2021). By applying the EBM to cross-sectional data from PWE, we aimed to answer two questions. Firstly, is there a characteristic order in which regional brain MRI morphometric changes develop in MTLE-HS? Secondly, is the accumulation of imaging changes related to clinical markers of disease duration or severity?

## *2. Materials and methods*

### *2.1 Data*

We analysed data from the ENIGMA-Epilepsy working group (Sisodiya et al., 2020) comprising imaging data from controls and people with epilepsy from 25 centres (**Table 1**). Each centre received approval from their local institutional review board or ethics committee. Written informed consent was provided according to local requirements. As previously described (Whelan et al., 2018), T1-weighted (T1W) brain MRI scans were acquired using 1.5T or 3T MRI scanners from different manufacturers and different imaging sequences. Brain scans were processed at each contributing centre using the same pipeline based on FreeSurfer Version 5.3.0 (Dale et al., 1999; Fischl, 2012). Diagnosis of left and right MTLE were made by an epilepsy specialist at each centre, based on seizure semiology and EEG findings. Presumed sclerosis of the hippocampus or the mesial temporal lobe was diagnosed according to established features on MRI (i.e., a T2-weighted or fluid-attenuated inversion recovery (FLAIR) scan). In some cases, HS was confirmed based on histology from resected tissue. A common set of 156 regional features was extracted based on the Desikan-Killiany atlas (Desikan et al., 2006): 68 measures for regional cortical thickness (CT), 68 measures of regional surface area (SA), two measures of hemispheric average CT, two measures of hemispheric SA, and 16 subcortical brain volumes as previously described in detail (Whelan et al., 2018). Since the initial study (Whelan et al., 2018), five new centres were added, providing an additional 244 subjects. Overall, the ENIGMA-Epilepsy dataset features pre-processed MRI scans from 1,625 controls as well as 446 left MTLE-HS and 358 right MTLE-HS patients. After segmentation quality assurance, certain regional brain measures were removed for some subjects in the acquired dataset (about 0.02% of the values). We removed subjects with more than ten missing values (66 subjects). Missing measures in the remaining subjects were imputed within each centre using a singular value decomposition (SVD)-based approach (Troyanskaya et al., 2001). Additionally, age, sex, case-control status, lateralization (left or right MTLE-HS), age at onset and duration of illness were available. Furthermore, drug-resistance status (defined as one or more seizures in the 12 months before MRI) was obtained for 408 MTLE-HS cases.

### *2.2 Data harmonization and confound adjustment*

Since ENIGMA-Epilepsy is a multi-centric study, the data are subject to centre-specific biases arising from various factors. Thus, all 156 regional brain measures were harmonized for centre

biases using NeuroCombat (Fortin et al., 2018; Johnson et al., 2007), while retaining variation originating from age, sex, intracranial volume (ICV) and diagnosis. Following the harmonization, the regional measures were adjusted for ICV, age, and sex using linear regression. As in previous work (Gleichgerrcht et al., 2021), the residuals for each regional measure plus the intercept of the model were used as confound-adjusted measures for the remaining analysis.

### *2.3 Ipsilateral and contralateral features*

Studies have shown unilateral and bilateral alterations of structural connectivity and structural measures in left and right MTLE-HS patients, with the ipsilateral regions being more strongly affected (Bonilha et al., 2015; Gleichgerrcht et al., 2021; Larivière et al., 2020; M. Liu et al., 2016). To estimate a progression pattern for MTLE-HS regardless of lateralization, we jointly analysed left and right MTLE-HS cases. Therefore, we replaced 'left' and 'right' with the 'ipsilateral' and 'contralateral' (e.g., left hemisphere is ipsilateral in left MTLE-HS and contralateral in right MTLE-HS). For the controls, we randomly sampled half as controls for left MTLE-HS, where left and right hemispheres were defined as ipsilateral and contralateral regions, respectively. Similarly, the remaining half acted as controls for right MTLE-HS with the hemispheres swapped. Overall, this enabled us to study brain regions commonly affected in both left and right MTLE-HS.

### *2.4 Brain Asymmetry Index features*

Previous studies (Park et al., 2021; Shah et al., 2019) have used the asymmetry of brain regions to model atrophy in people with MTLE-HS. The rationale is that contralateral brain regions of each subject act as a personalized healthy reference region (in cases where pathology manifests unilaterally) and therefore may act as an earlier, more sensitive marker, in the EBM. We computed the brain asymmetry index (BASI) for regional cortical thickness, surface area and volume as following ratio:

$$BASI = \frac{(ipsilateral - contralateral)}{(ipsilateral + contralateral)/2}$$

### *2.5 Feature selection*

First, we sought to identify brain regions with sufficient epilepsy-related atrophy to be used for progression modelling. We used a robust variant of Cohen's *d* (Cohen, 1962) between MTLE-HS cases and controls for all 234 features (78 ipsilateral, 78 contralateral and 78 BASI). Robust Cohen's *d* uses the median and mean absolute deviation in place of the mean and standard deviation, respectively, and is more resilient against outliers (Hampel, 1974). A medium effect size (robust Cohen's $|d|\geq 0.5$) was required for inclusion into disease progression modelling. We also evaluated a more lenient threshold (robust Cohen's $|d|\geq 0.4$).

### *2.6 Event-based modelling*

The selected regions were used as inputs to the EBM (Fonteijn et al., 2012). The EBM relies on two main assumptions: (i) biomarkers become abnormal sequentially; (ii) biomarkers follow a monotonic trajectory during disease progression, where an abnormal marker will not revert to a normal stage. Thus, the model assumes that for any given cross-sectional dataset a greater proportion of patients will show abnormalities for early-stage biomarkers, while fewer patients will also have abnormal later stage biomarkers. Further, the model requires distributions that define what normal and disease-specific measures look like for every biomarker. In practice, an overlap between the normal and disease-specific distributions for biomarkers is expected. We used a kernel density estimation-based (KDE) (Cao et al., 1994) mixture model that provides estimations of case and control distributions even when they are skewed or do not follow a parametric distribution (Firth et al., 2020). Next, the EBM determines the most likely ordering of biomarkers for the given dataset, as illustrated in **Figure 1**. Practically, the ordering is obtained using a maximum likelihood approach. Greedy ascent is used to initialise the sequence estimation and Markov Chain Monte Carlo (MCMC) sampling is used to perform the maximum likelihood estimation. The MCMC samples are used to derive a characteristic ordering of the events along with its variability. We used 10,000 iterations per chain during the greedy-ascent initialization and generated 500,000 MCMC samples. Finally, to generate a conservative, upper-bound estimate of the variability of the sequence, we combined the sequence estimation with bootstrapping (100 repeats) and generated positional variance diagrams from these bootstraps. The patient staging mechanism (Young et al., 2014) is then used to assign each of the control subjects and MTLE-HS cases to a disease stage ranging from zero (i.e., no abnormality) to an asymptotic endpoint, which equals the number of biomarkers selected for analysis (i.e., all biomarkers abnormal). To investigate whether the biomarker sequence is consistent in cases with left and right MTLE-HS, we trained EBMs for these two groups separately.

### *2.7 Association of EBM stages with duration of illness, age of onset and treatment response*

We hypothesized that subjects with advanced EBM-stages were more likely to have a longer duration of illness, earlier disease onset and are more likely to be drug-resistant. To determine whether individuals' EBM stage is related to illness duration or age of onset, we computed Spearman's rank correlations between EBM stage and the duration of illness (in years) at the time

of imaging and age of onset, respectively. Furthermore, we used the Mann-Whitney U test to test for a difference in EBM-assigned stage regarding drug-resistant status.

### *3. Results*

**Table 1** displays the overall cohort split by centre. On average, each centre contributed a range of individuals, ranging from young adults in their 20s to adults over 60 years (median 33.0 years; IQR 18.08 years). The binary sex distribution within the dataset was well balanced with a slight majority of women (56.0% of MTLE-HS patients and 55.9% of healthy controls). The duration of illness ranged from recently diagnosed to 68 years (median 20.0 years; IQR 24.0 years).

#### *3.1 Effect sizes of selected features*

The seven selected features (robust Cohen's $|d|\geq 0.5$) were ipsilateral hippocampal volume and its BASI, ipsilateral thalamic volume, cortical thickness of bilateral superior parietal gyrus, ipsilateral precuneus and ipsilateral lateral ventricle volume (**Supplementary Table S1**). **Figure 2** provides a visual representation of the effect sizes rendered using the ENIGMA toolbox (Larivière et al., 2021). Our mega-analysis replicated the finding of the original ENIGMA-Epilepsy meta-analysis (Whelan et al., 2018). Effect sizes (robust Cohen's *d*) ipsilateral to the seizure focus were stronger than those in the corresponding contralateral region for the surface area ($t$=4.01; $p$= 0.00033; $df$=33; paired t-test) but not for cortical thickness ($t$=1.95, $p$=0.06; $df$=33, paired t-test) nor for subcortical volumes ($t$=1.60; $p$= 0.15; $df$=7; paired t-test). Effect sizes for cortical thickness were stronger than effect sizes for surface area ($t$=8.08; $p$=1.09x$10^{-11}$; $df$=67; paired t-test). Use of the lower Cohen's *d* cut-off of 0.4 produced 12 additional features for EBM modelling (**Supplementary Table S1**).

#### *3.2 Sequence of abnormal biomarkers in left and right MTLE-HS*

The EBM estimated the sequence for the seven selected imaging biomarkers using the KDE mixture models (**Supplementary Figure S1**) and placed them in stages 0 to 7 (**Figure 3**). The bootstrapped version of the EBM placed reduced ipsilateral hippocampal volume and increased asymmetry in hippocampal volume at the beginning of the sequence. This was followed by decreased cortical thickness and decreased ipsilateral thalamic volume (**Figure 3**). We analysed left and right MTLE-HS cases separately, with similar progression patterns in both syndromes (**Supplementary Figure S2**). Reducing the inclusion threshold to Cohen's $|d|\geq 0.4$ led to 19 biomarkers and provided a more fine-grained staging, but with essentially the same progression sequence as in the original analysis (**Supplementary Figure S3**).

### *3.3 Cross-sectional distribution of patients across disease stages as defined by EBM*

We used the trained EBM to stage participants based on brain regions with structural alterations (Young et al., 2014): controls and PWE were assigned to stages zero to seven. Most of the MTLE-HS cases (71.1%) were staged at stage one or greater (**Figure 4**). However, a large proportion of MTLE-HS cases (28.9%) were staged at zero, indicating mild or non-detectable abnormality on T1W MRI. About 44.4% were assigned to stages one and two, reflecting reduced volume of the ipsilateral hippocampus and abnormal asymmetry in the hippocampus. The remaining MTLE-HS cases (26.7%) were staged beyond stage two, suggesting neocortical involvement, reduction of ipsilateral thalamic volume and increase in ipsilateral lateral ventricle volume. The distribution of stages differed between left and right MTLE-HS cases ($H$ = 7.35, $p$-value = 0.0067; Kruskal-Wallis test; **Supplementary Figure S4**).

Ipsilateral hippocampal volumes in cases at stage zero were significantly larger than in cases assigned to later stages ($t$=32.35, $p$ =7.77x10$^{-146}$, t-test; **Supplementary Figure S5**). Consequently, effect size of ipsilateral hippocampal volume was $d$=-0.31 and $d$=-2.09 for cases at stage zero and non-zero stages, respectively. In addition, cases assigned to EBM stages 3-7 exhibited reduced contralateral hippocampal volume compared to controls ($d$=-0.54), which was not observed in cases assigned to stage zero ($d$=-0.17) or stages 1-2 ($d$=0.16).

### *3.4 EBM stage is associated with duration of illness and with response to ASMs in MTLE patients.*

MTLE-HS patients assigned to early EBM stages showed a relatively shorter illness duration than those in later stages (**Figure 5**). Duration of illness and stages 0-7 were significantly correlated in all MTLE-HS cases (Spearman's $\rho$=0.293, $p$=7.03x10$^{-16}$). After excluding cases at stage zero, the correlation remained marginally significant (Spearman's $\rho$=0.099, $p$=0.024). Thus, the correlation is driven by the significant difference in duration of illness between EBM stage zero (mean: 15.7 years) and non-zero (mean: 25.1 years; $t$=-8.23, $p$=8.63x10$^{-16}$). The same pattern was observed for age of onset: EBM stage and age of onset were negatively correlated ($\rho$=-0.18, $p$=9.82x10$^{-7}$), but the effect vanished in the subset of cases at stages 1-7 ($\rho$=0.004, $p$=0.92). Age at onset was significantly later for stage zero cases compared to non-zero cases ($t$=5.69, $p$=1.75x10$^{-8}$). EBM

stages differed between MTLE-HS cases who were resistant ($N$=363) or responsive ($N$=45) to ASMs in the 12 months prior to MRI (AUC=0.589, $p$=0.043, Mann-Whitney U test).

## *4. Discussion*

We applied data-driven disease progression modelling to a large, multi-centre imaging study of epilepsy to characterize the progression of MTLE-HS. We identified a characteristic order of MRI morphometric changes originating in the ipsilateral hippocampus. We did not identify statistically significant correlations between the accumulation of imaging changes (EBM stages 1-7) and available clinical markers of disease duration or severity in this cohort.

For the progression modelling, we retained features exhibiting a medium effect size between cases and controls $|d|\geq 0.5$; and 0.4 for a sensitivity analysis (**Supplementary Table S1**). Our most interesting observation was a pattern of brain atrophy that appears to progress from the ipsilateral hippocampus to bilateral neocortical regions (e.g., precuneus and superior parietal lobule) as well as the bilateral thalamus (**Supplementary Figure S3**). Volume reduction and increased asymmetry in the hippocampus may represent a genetic predisposition to HS since hippocampal abnormalities have been frequently observed in healthy siblings of people with MTLE (Kobayashi et al., 2002; Long et al., 2020; Tsai et al., 2013; Vaughan et al., 2017), and an association was observed in a GWAS (Kasperavičiute et al., 2013). However, cortical thinning likely represents disease-related effects since these changes have not been reported in healthy siblings (Alhusaini et al., 2019). Furthermore, the progression pattern included decline in thalamic volume, which is a common feature in MTLE-HS (Bernhardt et al., 2012; Keller et al., 2008; Pulsipher et al., 2007; Seidenberg et al., 2008) and may be linked to the strong structural connectivity between the hippocampus and the thalamus (Bernasconi et al., 2004; Keller et al., 2008; Maller et al., 2019).

At first glance, it appears surprising that many MTLE-HS cases were assigned to stage zero despite the loss of hippocampal volume being one of the hallmark signs of MTLE-HS. Two factors contribute to this discrepancy. Firstly, the radiologic diagnosis of HS is based on multiple imaging sequences, whereas hippocampal atrophy, as defined on T1W images is only one component of HS (Jin et al., 2018). Secondly, even though we observed a large group effect size for hippocampal volume difference in the whole cohort ($d$=-1.76), there is significant variability in volume loss at the individual level. In fact, about half the subjects with HS exhibit hippocampal volume that is within the normal range (Coan et al., 2014); this is also the case in the ENIGMA-Epilepsy cohort (**Supplementary Figures S1 and S5**).

Duration of illness is typically used as a proxy for progression in cross-sectional studies (Bernhardt et al., 2009; Caciagli et al., 2017; McDonald et al., 2008). Moreover, within ENIGMA-Epilepsy (Whelan et al., 2018) changes in numerous neocortical regions, subcortical volumes as well as hippocampal volume were negatively correlated with duration of illness. However, these results were driven by epilepsies without HS: no correlations within the left MTLE-HS subgroup were found to be statistically significant; and within the right MTLE-HS group significant correlations were limited to the ipsilateral hippocampus, putamen, thalamus as well as the contralateral transverse temporal gyrus and the ipsilateral caudal middle frontal gyrus. Therefore, the marginal correlations between EBM stages 1-7 and duration of illness in subjects with MTLE-HS agrees with these earlier observations. Furthermore, Zhang et al. (2017) reported that measures of the ipsilateral hippocampus, the bilateral frontal lobes, and cerebellar hemispheres negatively correlated with duration of illness. However, in the same study, the lifetime number of seizures, another proxy for disease severity, was investigated and was correlated with atrophy in a different set of brain regions. Thus, either measure may capture different aspects of disease severity and the relationship between disease duration and atrophy may be more complex. Disease duration, and the other measures examined here are the most obvious and plausible factors to examine, and those most available, but may not be those that most influence the EBM-derived sequence of changes we detect.

Longitudinal studies of PWE reveal cortical atrophy beyond the expected range of normal aging (Alvim et al., 2016; Bernhardt et al., 2009; Coan et al., 2009; Liu et al., 2003). Moreover, recent longitudinal studies of people with focal epilepsy (Galovic et al., 2019, 2020) found progressive atrophy in the contralateral regions of the parietal and frontal lobes, which was also featured in our study when using the more lenient cutoff (**Supplementary Figure S3**). Overall, we find that our regional disease progression sequence, which is based on cross-sectional data, agrees with previous findings in longitudinal cohorts that show the progressive nature of atrophy in MTLE-HS (Bernhardt et al., 2009; Bernhardt et al., 2013; Caciagli et al., 2017). Contralateral hippocampal volume (d=-0.14) missed the inclusion threshold for the EBM. Thus, the analysis could not provide further insights on whether untreated unilateral HS will lead to bilateral HS. However, PWE assigned to later EBM stages did present with reduced volume in the contralateral

hippocampus, while this was not the case for PWE assigned to earlier stages, illustrating the potential of EBM.

The staging of individual MTLE-HS patients using the trained EBM allowed us to investigate associations with duration of illness and clinical markers such as ASM resistance. In agreement with Whelan et al. (2018) and Zhang et al. (2017), EBM-based stages (stage 0 to stage 7) and duration of illness were found to be correlated. However, this association was mainly driven by patients who were assigned to stage zero. Indeed, MTLE-HS cases assigned to EBM stage zero did not show pronounced changes in ipsilateral hippocampal volume compared to controls (**Supplementary Figure S5**) and as a group had shorter duration of illness and later age of onset than the other MTLE-HS cases. Of note, the fraction of stage zero MTLE-HS varied across centres (**Supplementary Figure S6**) and may reflect differences between regional practices and capabilities to detect and diagnose mesial temporal sclerosis or hippocampal sclerosis.

There were several limitations in our study. First, this ENIGMA-Epilepsy cohort is not a population-based cohort but represents data mostly from tertiary epilepsy centres and therefore the findings may not be generalisable to the overall epilepsy population. Also, within the ENIGMA-Epilepsy cohort, we observed sampling bias regarding availability of ASM response data (**Supplementary Table S2**): PWE with missing response data were younger, diagnosed more recently and had later age of onset. Second, although the results were robust under bootstrap validation, they would benefit from a validation in a longitudinal cohort. However, designing well-powered longitudinal studies in controls and patients is challenging, especially since drug-resistant TLE patients may eventually undergo epilepsy surgery (Caciagli et al., 2017). Third, clinical features such as lifelong ASM exposure were not available in the ENIGMA-Epilepsy dataset and would prove difficult to ascertain retrospectively but should be considered in future work. The use of specific ASMs may affect disease progression and, in some cases, even amplify tissue loss in epilepsy (Tondelli et al., 2020). Finally, our model could be improved by considering measures from diffusion MRI scans to understand the role of white matter abnormalities in disease progression (Hatton et al., 2020; Sisodiya et al., 2020).

In conclusion, we estimated a sequence of progressive pathology in MTLE-HS that can be used to assign patients to fine-grained, image-based disease stages. Beyond stage zero, the EBM staging

did not correlate with duration of illness, age of onset or drug-resistance. However, our EBM model trained on the ENIGMA-Epilepsy data can be used to stage MTLE-HS subjects in other cohorts with relevant clinical data and help establish connections between imaging-based progression staging and other clinical features such as the lifetime number of seizures and detailed information on ASM exposure.

# Acknowledgements

The ENIGMA-Epilepsy working group thanks and acknowledges all working group members (http://enigma.ini.usc.edu/ongoing/enigma-epilepsy/). A.A. holds an MRC eMedLab Medical Bioinformatics Career Development Fellowship; this work was partly supported by the Medical Research Council [grant number MR/L016311/ 1]. A.B. is supported by CIHR MOP-57840. B.Ber. acknowledges research support from NSERC (Discovery-1304413), CIHR (FDN-154298, PJT-174995), Azrieli Center for Autism Research of the Montreal Neurological Institute (ACAR-TACC), SickKids Foundation (NI17-039), the Helmholtz International BigBrain Analytics and Learning Laboratory (Hiball), the Tier-2 Canada Research Chairs program and salary support from FRQS (Chercheur Boursier Junior 1). C.D.W. is supported by Health Research Board of Ireland PhD scholarship. C.L.Y. is supported by FAPESP - BRAINN (2013/07599-3); CNPQ (403726/2016-6). C.R.M. is supported by NIH R01 NS065838; R21 NS107739. D.J.S. is supported by South African Medical Research Council. The UNICAMP research centre (Brazilian Institute of Neuroscience and Neurotechnology) was funded by FAPESP (São Paulo Research Foundation); Contract grant number 2013/07559-3. F.C. was supported by CNPq (Conselho Nacional de Pesquisa, Brazil), grant number 311231/2019-5. G.D.J. is supported by the National Health and Medical research council, the Australian Medical Research Future Fund with support from the Victorian State Government infrastructure fund. G.P.W. was supported by the MRC (G0802012, MR/M00841X/1). J.S.D. is supported by NIHR. Clinical Research Time Award and BRAIN Unit Infrastructure Award (Grant no: UA05) funded by Welsh Government through Health and Care Research Wales. L.M.A. has received funding from the European Union's Horizon 2020 research and innovation program under grant agreement No. 666992. L.Co. is supported by Mexican Council of Science and Technology (CONACYT 181508, 232676, 251216, and 280283); UNAM-DGAPA (IB201712). M.A. is supported by FAPESP 15/17066-0. M.E.M.-S. is supported by NIH funding. M.R. is supported by Medical Research Council programme grant (MR/K013998/1); Medical Research Council Centre for Neurodevelopmental Disorders (MR/N026063/1); NIHR Biomedical Research Centre at South London and Maudsely NHS Foundation Trust. N.Be. is supported by CIHR MOP-123520; CIHR MOP-130516. N.J. is supported in part by grants R01AG059874 and R01MH117601. N.K.F. is supported by DFG FO750/5-1. N.P.O. is a UKRI Future Leaders Fellow (MR/S03546X/1) and acknowledges funding

from the National Institute for Health Research University College London Hospitals Biomedical Research Centre. O.D. is supported by Finding A Cure for Epilepsy and Seizures (FACES). P.K. is supported by S10OD023696; R01EB015611. P.M. was supported by the PATE program (F1315030) of the University of Tübingen. P.M.T. is supported by NIH grants R01MH116147, P41EB015922, and R01AG058854. P.N.T. is supported by a UKRI Future Leaders Fellowship (MR/T04294X/1) Work developed within the framework of the DINOGMI Department of Excellence of MIUR 2018-2022 (legge 232 del 2016). R.H.T. is supported by Epilepsy Research UK. The Bern research centre was funded by Swiss National Science Foundation (grant 180365). R.W. received support from the Swiss League Against Epilepsy. S.E.M. is supported in part by NHMRC APP1172917. S.I.T. is supported, in part, by NIH grants R01MH116147, P41EB015922, and R01AG058854. S.L. is funded by CIHR. S.M. is supported by Italian Ministry of Health funding grant NET-2013-02355313. S.M.L. acknowledges support of an EPSRC Doctoral Training Partnership studentship (EP/R513143/1). S.S.K. is supported by Medical Research Council (MR/S00355X/1 and MR/K023152/1) and Epilepsy Research UK (1085). T.J.O. is supported by NHMRC Program Grant. T.W.O is supported by the Centre for Doctoral Training in Cloud Computing for Big Data (EP/L015358/1). The work was supported by the Epilepsy Society. This work was partly carried out at National Institute for Health Research (NIHR) University College London Hospitals Biomedical Research Centre, which receives a proportion of funding from the UK Department of Health's NIHR Biomedical Research Centres funding scheme.

## Conflicts of Interests/Disclosures

B.Ben. is the cofounder of AIRAmed GmbH, a company that offers brain segmentation. C.D.W. is an employee of Biogen Inc. D.J.S. has received research grants and/or consultancy honoraria from Lundbeck and Sun. K.H. has received honoraria and speaker fees from UCB, Eisai and GW Pharma L.V. reports research funding from Biogen Australia, Life Molecular Imaging and Eisai. N.K.F. received honoraria from Arvelle, Bial, Eisai, Philips/EGI, UCB. N.J. is MPI of a research grant from Biogen Inc for work unrelated to the contents of this manuscript. P.S. received speaker fees and advisory boards for Biomarin, Zogenyx, GW Pharmaceuticals; research funding by ENECTA BV, GW Pharmaceuticals, Kolfarma srl., Eisai. P.M.T. received a research grant from

Biogen, Inc., and was a paid consultant for Kairos Venture Capital, Inc., USA, for projects unrelated to this work. We confirm that we have read the Journal's position on issues involved in ethical publication and affirm that this report is consistent with those guidelines.

## Contributions

*Cohort PIs:* A.A., A.B., A.G., A.L., B.W., C.R.M., D.J.S., F.C., G.D.J., G.P.W., H.S., K.H., L.Co., M.R., N.Ba., N.Be., N.D., N.K.F., P.S., R.G., R.W., S.M., S.M.S., S.S.K., T.J.O., T.R.

*Contributed to the editing of the manuscript:* A.A., A.B., A.G., A.R., A.V., B.Ben., B.Ber., C.R.M., C.M., D.C.A., D.J.S., E.D., E.G., E.K., E.L., F.C., G.D.J., G.P.W., J.S.D., K.H., L.Ca., L.Co., L.M.A., L.V., M.A., M.G., M.M., N.Be., N.J., N.P.O., P.M.D., P.S., S.E.M., S.I.T., S.L., S.M.L., S.M.S., S.S.K., T.J.O., V.I.

*Imaging data collection:* A.B., A.R., B.Ben., B.W., C.d., C.D.W., C.L.Y., E.C., E.D., E.K., E.L., F.C., F.F., G.P.W., J.R., K.H., L.Co., L.V., M.A., M.E.M.-S., M.M., M.R., N.Be., O.D., P.M., P.M.D., P.S., R.G., R.H.T., S.A., S.S.K., Y.W.

*Imaging data analysis:* A.C., B.A.K.K., B.C., B.S., C.d., C.D.W., C.L.Y., D.C.A., E.D., J.R., K.H., L.M.A., L.V., M.C., M.D., M.L., M.R., M.T., N.J., P.K., P.M., P.N.T., R.G., R.K., S.F., S.M.L., S.S.K., T.W.O., Y.W.

*Core analysis group:* A.A., C.R.M., D.C.A., N.P.O., S.M.L., S.M.S.

*Core writing group:* A.A., C.R.M., D.C.A., N.P.O., S.M.L., S.M.S.

*Patient recruitment, phenotyping:* R.H.T.

*ENIGMA-Central:* P.M.T., S.I.T., N.J.

## References

Alhusaini, S., Doherty, C. P., Palaniyappan, L., Scanlon, C., Maguire, S., Brennan, P., Delanty, N., Fitzsimons, M., & Cavalleri, G. L. (2012). Asymmetric cortical surface area and morphology changes in mesial temporal lobe epilepsy with hippocampal sclerosis. *Epilepsia*, *53*(6), 995–1003. https://doi.org/10.1111/j.1528-1167.2012.03457.x

Alhusaini, S., Kowalczyk, M. A., Yasuda, C. L., Semmelroch, M. K., Katsurayama, M., Zabin, M., Zanão, T., Nogueira, M. H., Alvim, M. K. M., Ferraz, V. R., Tsai, M. H., Fitzsimons, M., Lopes-Cendes, I., Doherty, C. P., Cavalleri, G. L., Cendes, F., Jackson, G. D., & Delanty, N. (2019). Normal cerebral cortical thickness in first-degree relatives of temporal lobe epilepsy patients. *Neurology*, *92*(4), E351–E358. https://doi.org/10.1212/WNL.0000000000006834

Alvim, M. K. M., Coan, A. C., Campos, B. M., Yasuda, C. L., Oliveira, M. C., Morita, M. E., & Cendes, F. (2016). Progression of gray matter atrophy in seizure-free patients with temporal lobe epilepsy. *Epilepsia*, *57*(4), 621–629. https://doi.org/10.1111/epi.13334

Bernasconi, N., Duchesne, S., Janke, A., Lerch, J., Collins, D. L., & Bernasconi, A. (2004). Whole-brain voxel-based statistical analysis of gray matter and white matter in temporal lobe epilepsy. *NeuroImage*, *23*(2), 717–723. https://doi.org/10.1016/j.neuroimage.2004.06.015

Bernasconi, Neda, Natsume, J., & Bernasconi, A. (2005). Progression in temporal lobe epilepsy: Differential atrophy in mesial temporal structures. *Neurology*, *65*(2), 223–228. https://doi.org/10.1212/01.wnl.0000169066.46912.fa

Bernhardt, B. C., Worsley, K. J., Kim, H., Evans, A. C., Bernasconi, A., & Bernasconi, N. (2009). Longitudinal and cross-sectional analysis of atrophy in pharmacoresistant temporal lobe epilepsy. *Neurology*, *72*(20), 1747–1754. https://doi.org/10.1212/01.wnl.0000345969.57574.f5

Bernhardt, Boris C., Bernasconi, N., Kim, H., & Bernasconi, A. (2012). Mapping thalamocortical network pathology in temporal lobe epilepsy. *Neurology*, *78*(2), 129–136.

https://doi.org/10.1212/WNL.0b013e31823efd0d

Bernhardt, Boris C., Kim, H., & Bernasconi, N. (2013). Patterns of subregional mesiotemporal disease progression in temporal lobe epilepsy. *Neurology*, *81*(21), 1840–1847. https://doi.org/10.1212/01.wnl.0000436069.20513.92

Bonilha, L., Jensen, J. H., Baker, N., Breedlove, J., Nesland, T., Lin, J. J., Drane, D. L., Saindane, A. M., Binder, J. R., & Kuzniecky, R. I. (2015). The brain connectome as a personalized biomarker of seizure outcomes after temporal lobectomy. *Neurology*, *84*(18), 1846–1853. https://doi.org/10.1212/WNL.0000000000001548

Bonilha, L., Rorden, C., Appenzeller, S., Carolina Coan, A., Cendes, F., & Min Li, L. (2006). Gray matter atrophy associated with duration of temporal lobe epilepsy. *NeuroImage*, *32*(3), 1070–1079. https://doi.org/10.1016/j.neuroimage.2006.05.038

Caciagli, L., Bernasconi, A., Wiebe, S., Koepp, M. J., Bernasconi, N., & Bernhardt, B. C. (2017). A meta-Analysis on progressive atrophy in intractable temporal lobe epilepsy: Time is brain? *Neurology*, *89*(5), 506–516. https://doi.org/10.1212/WNL.0000000000004176

Cao, R., Cuevas, A., & González Manteiga, W. (1994). A comparative study of several smoothing methods in density estimation. *Computational Statistics and Data Analysis*, *17*(2), 153–176. https://doi.org/10.1016/0167-9473(92)00066-Z

Coan, A. C., Appenzeller, S., Li, L. M., & Cendes, F. (2009). Seizure frequency and lateralization affect progression of atrophy in temporal lobe epilepsy. *Neurology*, *73*(11), 834–842. https://doi.org/10.1212/WNL.0b013e3181b783dd

Coan, A. C., Kubota, B., Bergo, F. P. G., Campos, B. M., & Cendes, F. (2014). 3T MRI quantification of hippocampal volume and signal in mesial temporal lobe epilepsy improves detection of hippocampal sclerosis. *American Journal of Neuroradiology*, *35*(1), 77–83. https://doi.org/10.3174/ajnr.A3640

Cohen, J. (1962). The statistical power of abnormal-social pyschological research: A review. *Journal of Abnormal and Social Psychology*, *65*, 145–153.

Dale, A. M., Fischl, B., & Sereno, M. I. (1999). Cortical Surface-Based Analysis: I. Segmentation and Surface Reconstruction Anders. *NeuroImage*, *9*(2), 179–194. https://doi.org/10.1006/nimg.1998.0395

Dekker, I., Schoonheim, M. M., Venkatraghavan, V., Eijlers, A. J. C., Brouwer, I., Bron, E. E., Klein, S., Wattjes, M. P., Wink, A. M., Geurts, J. J. G., Uitdehaag, B. M. J., Oxtoby, N. P., Alexander, D. C., Vrenken, H., Killestein, J., Barkhof, F., & Wottschel, V. (2021). The

sequence of structural, functional and cognitive changes in multiple sclerosis. *NeuroImage: Clinical*, *29*(September 2020), 102550. https://doi.org/10.1016/j.nicl.2020.102550

Desikan, R. S., Ségonne, F., Fischl, B., Quinn, B. T., Dickerson, B. C., Blacker, D., Buckner, R. L., Dale, A. M., Maguire, R. P., Hyman, B. T., Albert, M. S., & Killiany, R. J. (2006). An automated labeling system for subdividing the human cerebral cortex on MRI scans into gyral based regions of interest. *NeuroImage*, *31*(3), 968–980. https://doi.org/10.1016/j.neuroimage.2006.01.021

Engel, J. J., Van Ness, P., Rasmussen, T., & Ojemann, L. (1993). Outcome with respect to epileptic seizures. In J. Engel (Ed.), *Surgical Treatment of the Epilepsies, Raven Press, New York* (2nd edn). Raven Press.

Eshaghi, A., Marinescu, R. V., Young, A. L., Firth, N. C., Prados, F., Jorge Cardoso, M., Tur, C., De Angelis, F., Cawley, N., Brownlee, W. J., De Stefano, N., Laura Stromillo, M., Battaglini, M., Ruggieri, S., Gasperini, C., Filippi, M., Rocca, M. A., Rovira, A., Sastre-Garriga, J., … Ciccarelli, O. (2018). Progression of regional grey matter atrophy in multiple sclerosis. *Brain*, *141*(6), 1665–1677. https://doi.org/10.1093/brain/awy088

Firth, N. C., Primativo, S., Brotherhood, E., Young, A. L., Yong, K. X. X., Crutch, S. J., Alexander, D. C., & Oxtoby, N. P. (2020). Sequences of cognitive decline in typical Alzheimer's disease and posterior cortical atrophy estimated using a novel event-based model of disease progression. *Alzheimer's and Dementia*, *16*(7), 965–973. https://doi.org/10.1002/alz.12083

Fischl, B. (2012). FreeSurfer. *NeuroImage*, *62*(2), 774–781. https://doi.org/10.1016/j.neuroimage.2012.01.021

Fonteijn, H. M., Modat, M., Clarkson, M. J., Barnes, J., Lehmann, M., Hobbs, N. Z., Scahill, R. I., Tabrizi, S. J., Ourselin, S., Fox, N. C., & Alexander, D. C. (2012). An event-based model for disease progression and its application in familial Alzheimer's disease and Huntington's disease. *NeuroImage*, *60*(3), 1880–1889. https://doi.org/10.1016/j.neuroimage.2012.01.062

Fortin, J. P., Cullen, N., Sheline, Y. I., Taylor, W. D., Aselcioglu, I., Cook, P. A., Adams, P., Cooper, C., Fava, M., McGrath, P. J., McInnis, M., Phillips, M. L., Trivedi, M. H., Weissman, M. M., & Shinohara, R. T. (2018). Harmonization of cortical thickness measurements across scanners and sites. *NeuroImage*, *167*(June 2017), 104–120. https://doi.org/10.1016/j.neuroimage.2017.11.024

Gabel, M. C., Broad, R. J., Young, A. L., Abrahams, S., Bastin, M. E., Menke, R. A. L., Al-

Chalabi, A., Goldstein, L. H., Tsermentseli, S., Alexander, D. C., Turner, M. R., Leigh, P. N., & Cercignani, M. (2020). Evolution of white matter damage in amyotrophic lateral sclerosis. *Annals of Clinical and Translational Neurology*, *7*(5), 722–732. https://doi.org/10.1002/acn3.51035

Galovic, M., de Tisi, J., McEvoy, A. W., Miserocchi, A., Vos, S. B., Borzi, G., Cueva Rosillo, J., Vuong, K. A., Nachev, P., Duncan, J. S., & Koepp, M. J. (2020). Resective surgery prevents progressive cortical thinning in temporal lobe epilepsy. *Brain : A Journal of Neurology*, *143*(11), 3262–3272. https://doi.org/10.1093/brain/awaa284

Galovic, M., Van Dooren, V. Q. H., Postma, T. S., Vos, S. B., Caciagli, L., Borzì, G., Cueva Rosillo, J., Vuong, K. A., De Tisi, J., Nachev, P., Duncan, J. S., & Koepp, M. J. (2019). Progressive Cortical Thinning in Patients with Focal Epilepsy. *JAMA Neurology*, *76*(10), 1230–1239. https://doi.org/10.1001/jamaneurol.2019.1708

Gleichgerrcht, E., Munsell, B. C., Alhusaini, S., Alvim, M. K. M., Bargalló, N., Bender, B., Bernasconi, A., Bernasconi, N., Bernhardt, B., Blackmon, K., Caligiuri, M. E., Cendes, F., Concha, L., Desmond, P. M., Devinsky, O., Doherty, C. P., Domin, M., Duncan, J. S., Focke, N. K., … Wiest, R. (2021). Artificial intelligence for classification of temporal lobe epilepsy with ROI-level MRI data: A worldwide ENIGMA-Epilepsy study. *NeuroImage: Clinical*, *31*(July). https://doi.org/10.1016/j.nicl.2021.102765

Hampel, F. R. (1974). The influence curve and its role in robust estimation. *Journal of the American Statistical Association*, *69*(346), 383–393. https://doi.org/10.1080/01621459.1974.10482962

Hatton, S. N., Huynh, K. H., Bonilha, L., Abela, E., Alhusaini, S., Altmann, A., Alvim, M. K. M., Balachandra, A. R., Bartolini, E., Bender, B., Bernasconi, N., Bernasconi, A., Bernhardt, B., Bargallo, N., Caldairou, B., Caligiuri, M. E., Carr, S. J. A., Cavalleri, G. L., Cendes, F., … McDonald, C. R. (2020). White matter abnormalities across different epilepsy syndromes in adults: An ENIGMA-Epilepsy study. *Brain*, *143*(8), 2454–2473. https://doi.org/10.1093/brain/awaa200

Jin, B., Krishnan, B., Adler, S., Wagstyl, K., Hu, W., Jones, S., Najm, I., Alexopoulos, A., Zhang, K., Zhang, J., Ding, M., Wang, S., & Wang, Z. I. (2018). Automated detection of focal cortical dysplasia type II with surface-based magnetic resonance imaging postprocessing and machine learning. *Epilepsia*, *59*(5), 982–992. https://doi.org/10.1111/epi.14064

Johnson, W. E., Li, C., & Rabinovic, A. (2007). Adjusting batch effects in microarray expression

data using empirical Bayes methods. *Biostatistics*, *8*(1), 118–127. https://doi.org/10.1093/biostatistics/kxj037

Kasperavičiute, D., Catarino, C. B., Matarin, M., Leu, C., Novy, J., Tostevin, A., Leal, B., Hessel, E. V. S., Hallmann, K., Hildebrand, M. S., Dahl, H. H. M., Ryten, M., Trabzuni, D., Ramasamy, A., Alhusaini, S., Doherty, C. P., Dorn, T., Hansen, J., Krämer, G., … Sisodiya, S. M. (2013). Epilepsy, hippocampal sclerosis and febrile seizures linked by common genetic variation around SCN1A. *Brain*, *136*(10), 3140–3150. https://doi.org/10.1093/brain/awt233

Keller, S. S., & Roberts, N. (2008). Voxel-based morphometry of temporal lobe epilepsy: An introduction and review of the literature. *Epilepsia*, *49*(5), 741–757. https://doi.org/10.1111/j.1528-1167.2007.01485.x

Kobayashi, E., Li, L. M., Lopes-Cendes, I., & Cendes, F. (2002). Magnetic resonance imaging evidence of hippocampal sclerosis in asymptomatic, first-degree relatives of patients with familial mesial temporal lobe epilepsy. *Archives of Neurology*, *59*(12), 1891–1894. https://doi.org/10.1001/archneur.59.12.1891

Larivière, S., Bernasconi, A., Bernasconi, N., & Bernhardt, B. C. (2020). Connectome biomarkers of drug-resistant epilepsy. *Epilepsia*. https://doi.org/10.1111/epi.16753

Larivière, S., Paquola, C., Park, B. yong, Royer, J., Wang, Y., Benkarim, O., Vos de Wael, R., Valk, S. L., Thomopoulos, S. I., Kirschner, M., Lewis, L. B., Evans, A. C., Sisodiya, S. M., McDonald, C. R., Thompson, P. M., & Bernhardt, B. C. (2021). The ENIGMA Toolbox: multiscale neural contextualization of multisite neuroimaging datasets. *Nature Methods*, *18*(7), 698–700. https://doi.org/10.1038/s41592-021-01186-4

Liu, M., Bernhardt, B. C., Hong, S. J., Caldairou, B., Bernasconi, A., & Bernasconi, N. (2016). The superficial white matter in temporal lobe epilepsy: A key link between structural and functional network disruptions. *Brain*, *139*(9), 2431–2440. https://doi.org/10.1093/brain/aww167

Liu, R. S. N., Lemieux, L., Bell, G. S., Hammers, A., Sisodiya, S. M., Bartlett, P. A., Shorvon, S. D., Sander, J. W. A. S., & Duncan, J. S. (2003). Progressive neocortical damage in epilepsy. *Annals of Neurology*, *53*(3), 312–324. https://doi.org/10.1002/ana.10463

Long, L., Galovic, M., Chen, Y., Postma, T., Vos, S. B., Xiao, F., Wu, W., Song, Y., Huang, S., Koepp, M., & Xiao, B. (2020). Shared hippocampal abnormalities in sporadic temporal lobe epilepsy patients and their siblings. *Epilepsia*, *61*(4), 735–746. https://doi.org/10.1111/epi.16477

Maller, J. J., Welton, T., Middione, M., Callaghan, F. M., Rosenfeld, J. V., & Grieve, S. M. (2019). Revealing the Hippocampal Connectome through Super-Resolution 1150-Direction Diffusion MRI. *Scientific Reports*, *9*(1), 1–13. https://doi.org/10.1038/s41598-018-37905-9

McDonald, C. R., Hagler, D. J., Ahmadi, M. E., Tecoma, E., Iragui, V., Gharapetian, L., Dale, A. M., & Halgren, E. (2008). Regional neocortical thinning in mesial temporal lobe epilepsy. *Epilepsia*, *49*(5), 794–803. https://doi.org/10.1111/j.1528-1167.2008.01539.x

Oxtoby, N. P., Leyland, L.-A., Aksman, L. M., Thomas, G. E. C., Bunting, E. L., Wijeratne, P. A., Young, A. L., Zarkali, A., Tan, M. M. X., Bremner, F. D., Keane, P. A., Morris, H. R., Schrag, A. E., Alexander, D. C., & Weil, R. S. (2021). Sequence of clinical and neurodegeneration events in Parkinson's disease progression. *Brain*, 1–14. https://doi.org/10.1093/brain/awaa461

Park, B., Lariviere, S., Rodriguez-Cruces, R., Royer, J., Tavakol, S., Wang, Y., Caciagli, L., Caligiuri, M. E., Gambardella, A., Concha, L., Keller, S., Cendes, F., Alvim, M. K. M., Yasuda, C., Bonilha, L., Gleichgerrcht, E., Focke, N., Kreilkamp, B. A. K., Domin, M., … Bernhardt, B. (2021). *Topographic divergence of atypical cortical asymmetry and regional atrophy patterns in temporal lobe epilepsy: a worldwide enigma study*. accepted in Brain. http://europepmc.org/abstract/PPR/PPR319831%0Ahttps://doi.org/10.1101/2021.04.30.442117

Pulsipher, D. T., Seidenberg, M., Morton, J. J., Geary, E., Parrish, J., & Hermann, B. (2007). MRI volume loss of subcortical structures in unilateral temporal lobe epilepsy. *Epilepsy Behav*, *11*(3), 442–449. https://doi.org/10.1016/j.yebeh.2007.08.007

Seidenberg, M., Hermann, B., Pulsipher, D., Morton, J., Parrish, J., Geary, E., & Guidotti, L. (2008). Thalamic atrophy and cognition in unilateral temporal lobe epilepsy. *Journal of the International Neuropsychological Society*, *14*(3), 384–393. https://doi.org/10.1017/S1355617708080399

Shah, P., Bassett, D. S., Wisse, L. E. M., Detre, J. A., Stein, J. M., Yushkevich, P. A., Shinohara, R. T., Elliott, M. A., Das, S. R., & Davis, K. A. (2019). Structural and functional asymmetry of medial temporal subregions in unilateral temporal lobe epilepsy: A 7T MRI study. *Human Brain Mapping*, *40*(8), 2390–2398. https://doi.org/10.1002/hbm.24530

Sisodiya, S. M., Whelan, C. D., Hatton, S. N., Huynh, K., Altmann, A., Ryten, M., Vezzani, A., Caligiuri, M. E., Labate, A., Gambardella, A., Ives-Deliperi, V., Meletti, S., Munsell, B. C., Bonilha, L., Tondelli, M., Rebsamen, M., Rummel, C., Vaudano, A. E., Wiest, R., …

McDonald, C. R. (2020). The ENIGMA-Epilepsy working group: Mapping disease from large data sets. *Human Brain Mapping*, *May*, 1–16. https://doi.org/10.1002/hbm.25037

Tondelli, M., Vaudano, A. E., Sisodiya, S. M., & Meletti, S. (2020). Valproate Use Is Associated With Posterior Cortical Thinning and Ventricular Enlargement in Epilepsy Patients. *Frontiers in Neurology*, *11*(July). https://doi.org/10.3389/fneur.2020.00622

Troyanskaya, O., Cantor, M., Sherlock, G., Brown, P., Hastie, T., Tibshirani, R., Botstein, D., & Altman, R. B. (2001). Missing value estimation methods for DNA microarrays. *Bioinformatics*, *17*(6), 520–525. https://doi.org/10.1093/bioinformatics/17.6.520

Tsai, M.-H., Pardoe, H. R., Perchyonok, Y., Fitt, G. J., Scheffer, I. E., Jackson, G. D., & Berkovic, S. F. (2013). Etiology of hippocampal sclerosis: Evidence for a predisposing familial morphologic anomaly. *Neurology*, *81*(2), 144–149. https://doi.org/10.1212/wnl.0b013e31829a33ac

Vaughan, D. N., Raffelt, D., Curwood, E., Tsai, M. H., Tournier, J. D., Connelly, A., & Jackson, G. D. (2017). Tract-specific atrophy in focal epilepsy: Disease, genetics, or seizures? *Annals of Neurology*, *81*(2), 240–250. https://doi.org/10.1002/ana.24848

Whelan, C. D., Altmann, A., Botía, J. A., Jahanshad, N., Hibar, D. P., Absil, J., Alhusaini, S., Alvim, M. K. M., Auvinen, P., Bartolini, E., Bergo, F. P. G., Bernardes, T., Blackmon, K., Braga, B., Caligiuri, M. E., Calvo, A., Carr, S. J., Chen, J., Chen, S., … Sisodiya, S. M. (2018). Structural brain abnormalities in the common epilepsies assessed in a worldwide ENIGMA study. *Brain*, *141*(2), 391–408. https://doi.org/10.1093/brain/awx341

Young, A. L., Oxtoby, N. P., Daga, P., Cash, D. M., Fox, N. C., Ourselin, S., Schott, J. M., & Alexander, D. C. (2014). A data-driven model of biomarker changes in sporadic Alzheimer's disease. *Brain*, *137*(9), 2564–2577. https://doi.org/10.1093/brain/awu176

Zhang, Z., Liao, W., Xu, Q., Wei, W., Zhou, H. J., Sun, K., Yang, F., Mantini, D., Ji, X., & Lu, G. (2017). Hippocampus-associated causal network of structural covariance measuring structural damage progression in temporal lobe epilepsy. *Human Brain Mapping*, *38*(2), 753–766. https://doi.org/10.1002/hbm.23415

# Figure Legends

*Figure 1. EBM workflow:* A set of k biomarkers and case-control status are provided for each subject. Then, mixture modelling is used to estimate distributions of the biomarkers in cases and controls, respectively. The maximum likelihood sequence (i.e., optimal ordering) of the *k* biomarkers is estimated using MCMC with 500,000 iterations. The MCMC sequence is initialized using 10 random starting solutions and a greedy ascent run for 10,000 iterations. Finally, in a third step, we used 100 bootstrap samples to determine the uncertainty and variability of the sequence.

*Figure 2: Regional differences in MTLE-HS compared to Controls.* Effect size between MTLE-HS cases and controls measured as *robust* Cohens' *d* for Surface Area, Cortical Thickness and Volumes depicted ipsilateral or contralateral to the seizure focus (top three rows). The bottom two rows depict effect sizes for asymmetry features.

*Figure 3. Sequential Accumulation of Pathology in MTLE-HS:* Data-driven sequence of atrophy or increased asymmetry of brain regions: Colour intensity in the positional variance diagram (PVD) represents the proportion of certainty (0.0 in white to 1.0 in dark blue) in which biomarkers (*y*-axis) appear in a particular position (x-axis) in the event order obtained through bootstrapping. CT=cortical thickness, V=Volume, BASI=Brain Asymmetry Index, I=ipsilateral, C=contralateral.

*Figure 4. EBM Stage Distribution:* Histogram showing stages (*x*-axis) assigned to controls and MTLE-HS patients and the corresponding count (*y*-axis). Stage 0 is assigned to subjects with no statistically detectable abnormal regional brain measure based on the T1W MRI scans. EBM places subjects with abnormal features progressively, such that subjects in stage 7 exhibit abnormality in all seven regional measures.

*Figure 5. Distribution of duration of illness per EBM stage:* Violin plots showing distribution of duration of illness (in years) of corresponding EBM stages 0-7 of MTLE-HS patients. MTLE-HS cases assigned to EBM stage 0 showed a shorter duration of illness compared to cases assigned to the remaining EBM stages.

# Tables

*Table 1. Cohort overview:* Table showing individual cohort demographics including age, number of left and right MTLE-HS, controls as well as age of onset and duration of illness for MTLE-HS patients.

| Centre | Age controls (Mean ± SD) | Age cases (Mean ± SD) | Age of onset (Mean ± SD) | Duration of illness (Mean ± SD) | Female controls | Female cases | Total controls | Total cases | L MTLE-HS cases | R MTLE-HS cases | Total *n* |
|---|---|---|---|---|---|---|---|---|---|---|---|
| Bern | 32.5± 9.39 | 31.3 ± 9.09 | N/A | N/A | 41 | 9 | 78 | 18 | 10 | 8 | 96 |
| Bonn | 40.4± 13.79 | 40.2 ± 13.37 | 17.1 ± 12.14 | 23 ± 14.16 | 41 | 62 | 80 | 112 | 74 | 38 | 192 |
| CUBRIC | 28± 8.17 | N/A | N/A | N/A | 34 | 0 | 48 | 0 | 0 | 0 | 48 |
| EKUT | 35.3± 12.33 | N/A | N/A | N/A | 9 | 0 | 18 | 0 | 0 | 0 | 18 |
| EPICZ | 38.8± 11.08 | 39.7 ± 9.11 | 18.1 ± 14.15 | 21.6 ± 13.48 | 59 | 26 | 116 | 46 | 19 | 27 | 162 |
| EPIGEN_3T | 34.7± 9.37 | 40.4 ± 6.28 | 21.8 ± 13.16 | 18.5 ± 11.98 | 30 | 6 | 70 | 13 | 8 | 5 | 83 |
| Florence | 32.2± 8.84 | N/A | N/A | N/A | 14 | 0 | 30 | 0 | 0 | 0 | 30 |
| Genova | 25.2± 8.23 | N/A | N/A | N/A | 8 | 1 | 20 | 1 | 0 | 1 | 21 |
| Greifswald | 26.3± 7.48 | N/A | N/A | N/A | 59 | 0 | 99 | 0 | 0 | 0 | 99 |
| HFHS | N/A | 40.4 ± 14.85 | 10.4 ± 12.96 | 25.4 ± 14.44 | 0 | 15 | 0 | 20 | 9 | 11 | 20 |
| IDIBAPS | 33.1± 5.99 | 37.4 ± 9.94 | 17.7 ± 12.79 | 18.8 ± 9.97 | 29 | 29 | 52 | 53 | 17 | 36 | 105 |
| KCL_CNS | 31.7± 8.4 | 41 ± 9.57 | 17.5 ± 14.16 | 25.2 ± 16.97 | 54 | 11 | 101 | 15 | 6 | 9 | 116 |
| KCL_CRF | 28.7± 8.29 | 37.8± 11.52 | 22.6 ± 12.34 | 15.2 ± 8.04 | 16 | 1 | 26 | 5 | 3 | 2 | 31 |
| KUOPIO | 25.2± 1.55 | 41.1± 11.06 | 23.3 ± 18.23 | 17.8 ± 17.02 | 33 | 5 | 67 | 9 | 0 | 9 | 76 |

| | | | | | | | | | | | |
|---|---|---|---|---|---|---|---|---|---|---|---|
| MICA | 31.9± 4.77 | 38.9± 13.12 | 23.4 ± 11.71 | 15.7 ± 14.58 | 18 | 7 | 38 | 14 | 12 | 2 | 52 |
| MNI | 30.7± 7.38 | 33.6± 9.53 | 17.3 ± 10.57 | 16.3 ± 11.4 | 22 | 48 | 46 | 83 | 45 | 38 | 129 |
| MUSC | 54.9± 8.4 | 33.5± 12.73 | 15.4 ± 12.34 | 18.2 ± 12.79 | 45 | 17 | 58 | 27 | 21 | 6 | 85 |
| NYU | 30.1± 10.36 | 33.8± 9.31 | 14.1 ± 8.04 | 20.2 ± 14.44 | 62 | 12 | 118 | 19 | 8 | 11 | 137 |
| RMH | 38.8± 20.44 | 39.6± 15.59 | 27.1 ± 17.69 | 12.4 ± 13.23 | 11 | 13 | 27 | 35 | 22 | 13 | 62 |
| UCL | 37.7± 12.4 | 39.5± 11.29 | 11.8 ± 8.72 | 27.7 ± 15.12 | 17 | 21 | 29 | 37 | 24 | 13 | 66 |
| UCSD | 36.9± 15.1 | 39.2± 12.53 | 15.6 ± 12.44 | 24.3 ± 17.82 | 16 | 15 | 37 | 26 | 16 | 10 | 63 |
| UMG | 34.7± 10.26 | 40.6± 12.49 | 15.4 ± 14.04 | 23.9 ± 18.49 | 12 | 12 | 21 | 20 | 10 | 10 | 41 |
| UNAM | 33.2± 12.29 | 34.4± 12.47 | 15.5 ± 13.84 | 18.8 ± 13.16 | 25 | 12 | 35 | 20 | 10 | 10 | 55 |
| UNICAMP | 34.4± 10.47 | 42.7± 8.33 | 11.4 ± 9.6 | 31.3 ± 12.13 | 249 | 113 | 398 | 191 | 107 | 84 | 589 |
| XMU | 31.5± 7 | 28.2± 8.45 | 17.2 ± 12.06 | 11.3 ± 8.02 | 4 | 15 | 13 | 40 | 25 | 15 | 53 |
| **Total** | **33.8 ± 11.45** | **38.5 ± 11.44** | **15.9 ± 12.4** | **22.7 ± 14.39** | **908** | **450** | **1625** | **804** | **446** | **358** | **2429** |

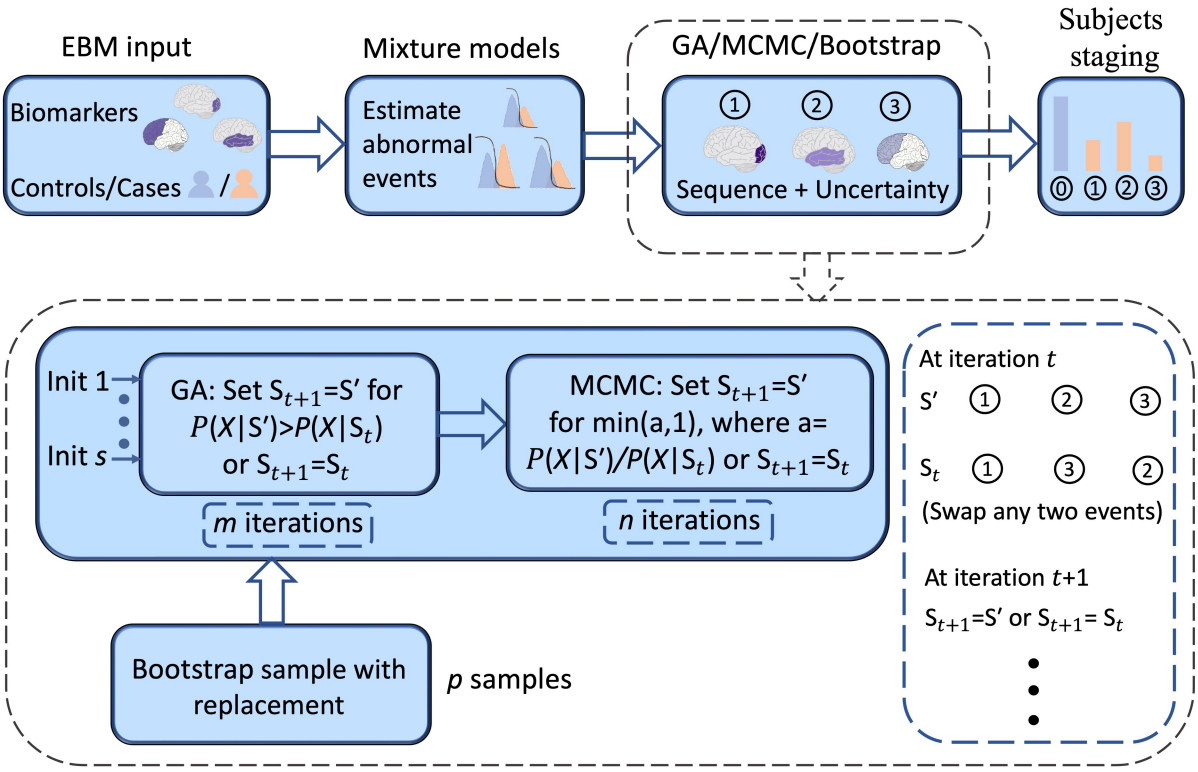


epi_17316_f1.tiff

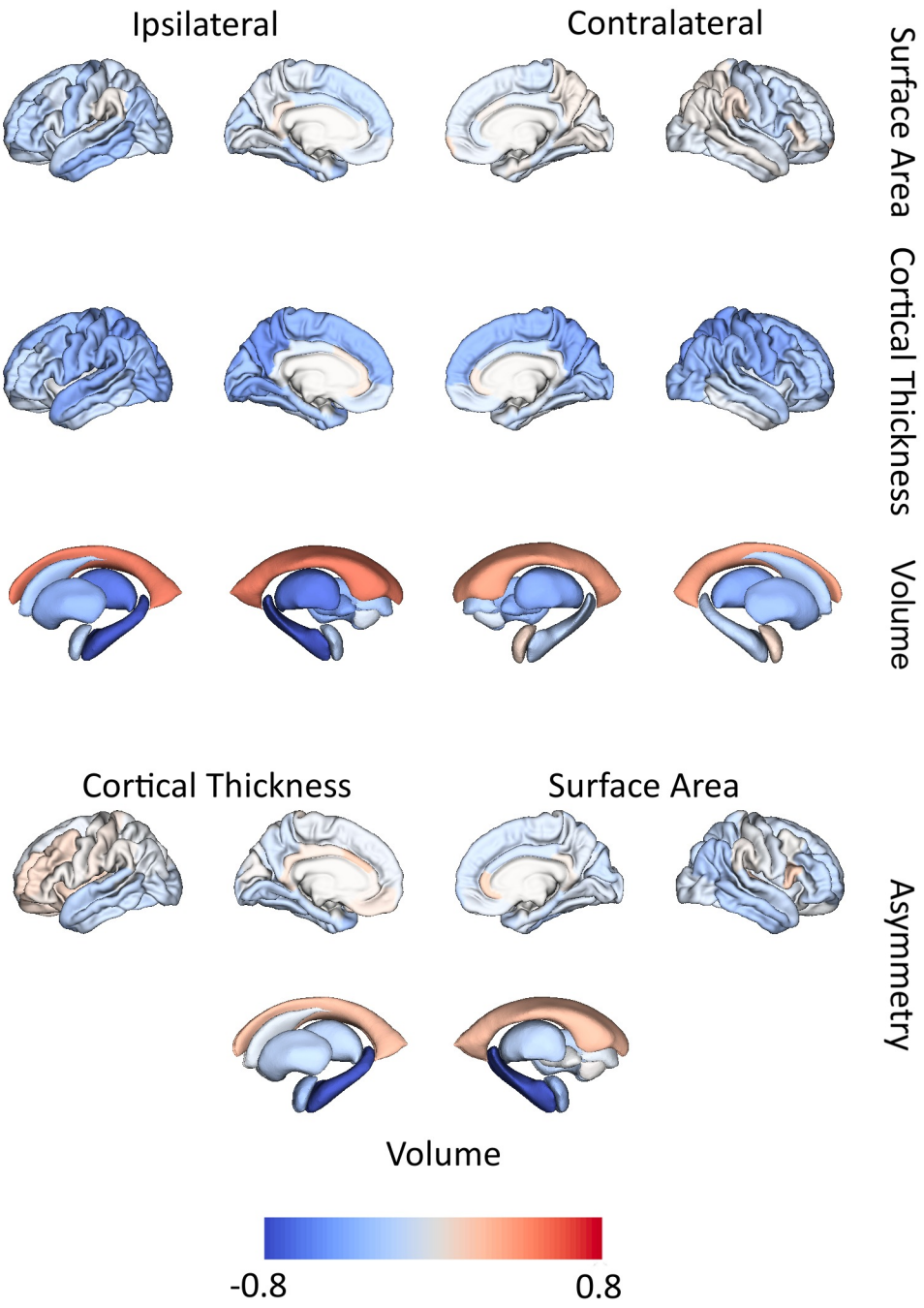


epi_17316_f2.tiff

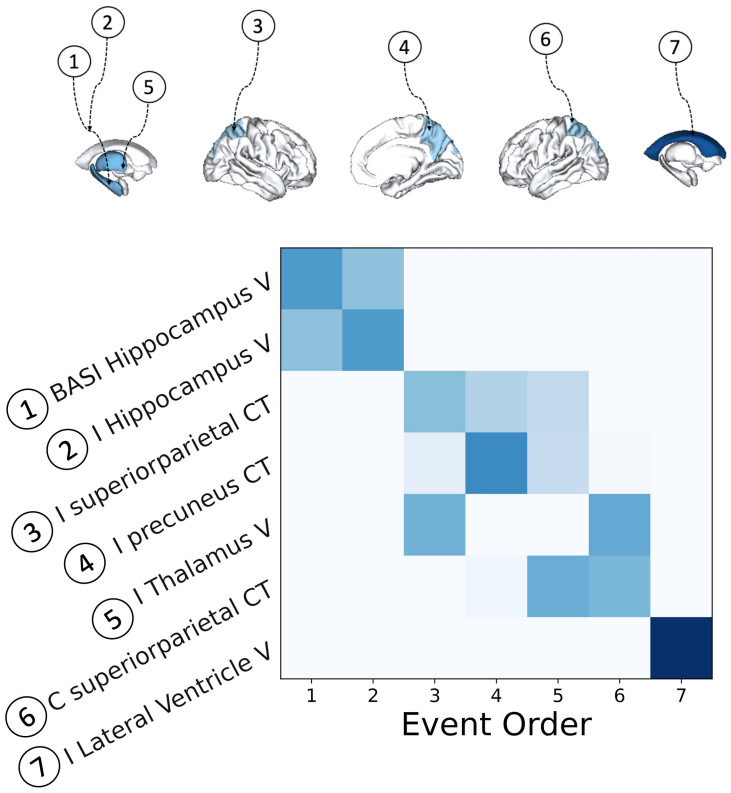


epi_17316_f3.tiff

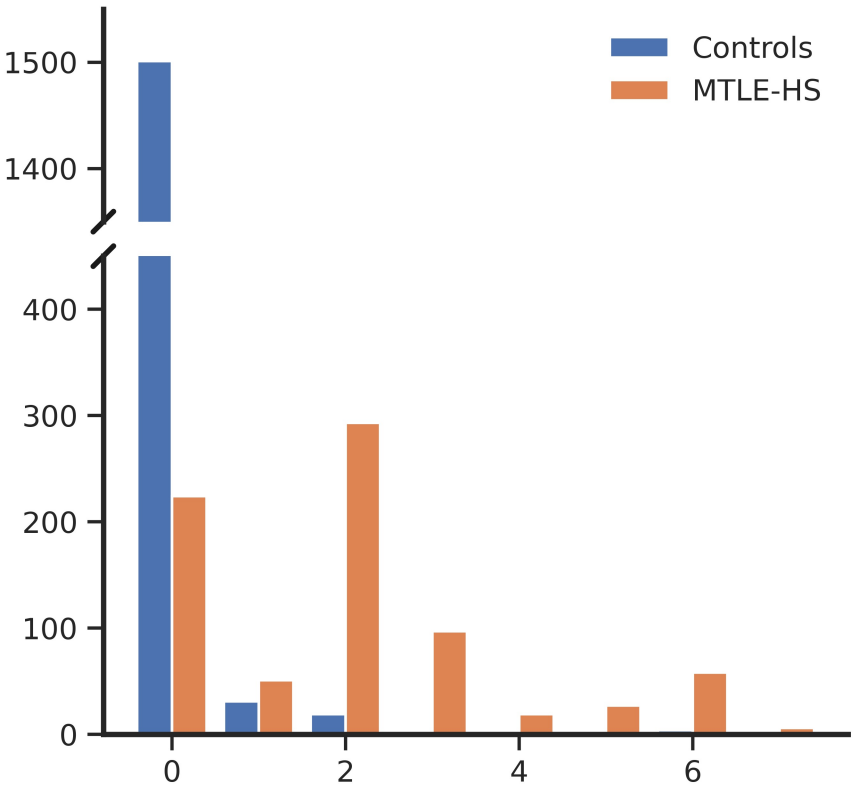


epi_17316_f4.tiff

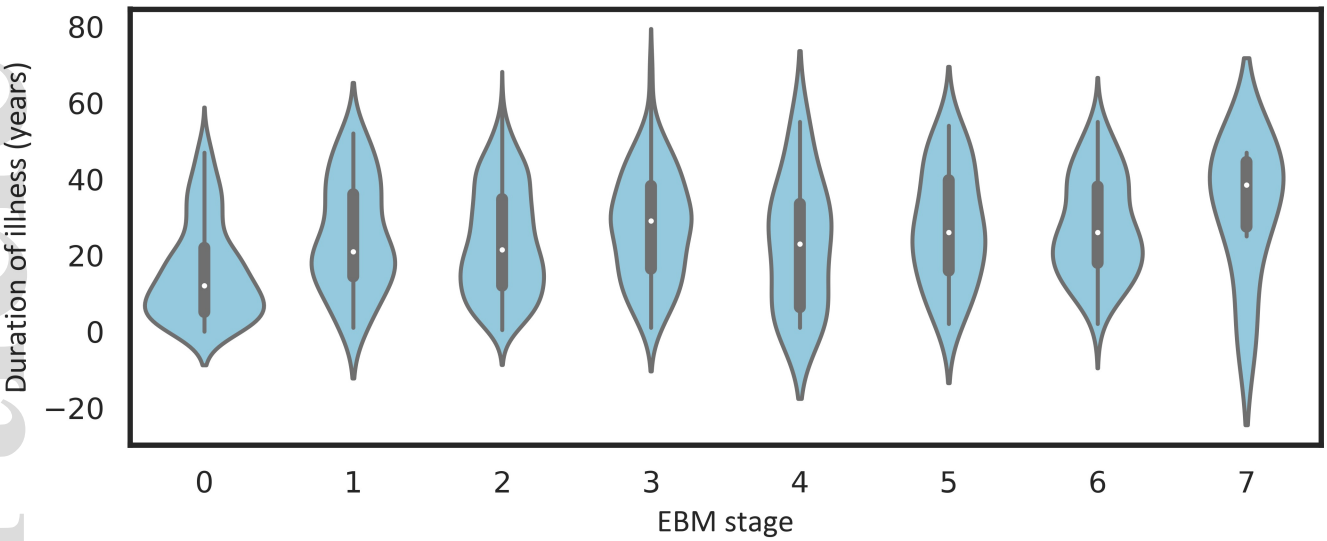


epi_17316_f5.tiff